# Multi-location laser ignition using a spatial light modulator towards improving automotive gasoline engine combustion stability and power generated

**Zheng Kuang[1*], Elliott Lyon[1], Hua Cheng[2], Vincent Page[2], Tom Shenton[2], Geoff Dearden[1]**
[1] *Laser Group, School of Engineering, University of Liverpool, Liverpool L69 3GQ, UK*
[2] *Powertrain Control Group, School of Engineering, University of Liverpool, Liverpool L69 3GH, UK*
**Corresponding Author: Z.Kuang@liverpool.ac.uk or kz518@msn.com*

**Abstract:** We report on a study into multi-location laser ignition (LI) with a Spatial Light Modulator (SLM), to improve the performance of a single cylinder automotive gasoline engine. Three questions are addressed: i/ How to deliver a multi-beam diffracted pattern into an engine cylinder, through a small opening, while avoiding clipping? ii/ How much incident energy can a SLM handle (optical damage threshold) and how many simultaneous beam foci could thus be created?; iii/ Would the multi-location sparks created be sufficiently intense and stable to ignite an engine and, if so, what would be their effect on engine performance compared to single-location LI? Answers to these questions were determined as follows. Multi-beam diffracted patterns were created by applying computer generated holograms (CGHs) to the SLM. An optical system for the SLM was developed via modelling in ZEMAX, to cleanly deliver the multi-beam patterns into the combustion chamber without clipping. Optical damage experiments were carried out on Liquid Crystal on Silicon (LCoS) samples provided by the SLM manufacturer and the maximum safe pulse energy to avoid SLM damage found to be 60 mJ. Working within this limit, analysis of the multi-location laser induced sparks showed that diffracting into three identical beams gave slightly insufficient energy to guarantee 100% sparking, so subsequent engine experiments used 2 equal energy beams laterally spaced by 4mm. The results showed that dual-location LI gave more stable combustion and higher engine power output than single-location LI, for increasingly lean air-fuel mixtures. The paper concludes by a discussion of how these results may be exploited.

**Keywords:** laser ignition, spatial light modulator, computer generated hologram, automotive gasoline engine, multi-location laser-induced spark.

## 1. Introduction

Engine ignition systems with electric spark plugs have been developed for the automobile industry for over a century. However, they offer only limited possibilities for optimizing engine efficiency, due to the fixed position and protrusion of their electrodes within the cylinder, which can quench the flame kernel. Recent research on laser ignition (LI) of air–fuel mixtures in internal combustion (IC) engines has revealed a number of potential advantages over conventional electrical spark ignition (SI) [1–5]. LI offers, in principle, the potential to deposit ignition energy at any location, including multiple points [6–8]. Other benefits foreseen include reduced emissions, faster ignition, more stable combustion, lower idle speeds and better cold engine performance. However, challenges remain, self-cleaning of the window into the cyclinder has not been demonstrated over long time periods, and the cost of the laser system needed is prohibitively high. Tauer et al. [9], Morsy et al. [10] and Dearden et al. [11] recently reviewed progress in research on laser ignited engines. Previous work on LI of IC engines found that simultaneously igniting in more than one location resulted in more stable and faster combustion [7]. Two previous attempts to create laser induced sparks in multiple locations for engine ignition were a complex arrangement of external conical cavities [7] and the use of three independent lines to pump a passively Q-switched Nd:YAG/Cr4+ laser cavity [8]. These were able to generate two and three foci, respectively, but only at fixed locations within the combustion chamber. We recently reported on an optical technique for multi-location spark generation in air using a spatial light modulator (SLM), for potential use in LI [12]. There, several sparks with arbitrary spacing in 3-dimensions were created by variable diffraction of a single pulsed laser beam and its transmission through a lens. However, before the benefits of the method could be properly evaluated on a test engine, the following questions were technical challenges to be addressed: i/ How to deliver a multi-beam diffracted pattern through a small opening into an engine cylinder, while avoiding clipping? ii/ How much incident energy can a SLM handle (optical damage threshold) and how many simultaneous beam

foci could thus be created?; iii/ Would the multi-location sparks created be sufficiently intense and stable to ignite an engine and, if so, what would be their effect on engine performance compared to single-location LI? This study firstly addresses each of these three questions. To address i/, we design and develop an optical system set-up incorporating the SLM, which aims to avoid clipping of the multi-beam pattern along its path into the combustion chamber. This was challenging, given the spatially diffracted beams must be carefully aligned and cleanly transmitted through the internal bore (minimum diameter 6 mm) of an optical plug, which replaces the SI plug and is vibrating with the engine, before final focusing into the cylinder. To address ii/, an experiment was carried out to assess the optical damage threshold of Liquid Crystal on Silicon (LCoS) samples provided by the SLM manufacturer. Here, the aim was to determine a maximum safe energy that could be applied to the SLM, and hence the energy available to distribute into multiple beams. To address iii/, based on the upper safe limit of energy derived from ii/, experiments were performed to analyse the stability of laser induced sparks generated in multiple foci by the SLM. The aim was to determine the minimum energy per foci needed for spark creation and thus how many beams with sufficient energy could be generated (under the specific optical conditions). The study then goes further to apply this SLM based technique to a single cylinder automotive gasoline IC engine and to evaluate the effect on engine performance of multi-location LI, comparing in this case the results for dual-location and single location LI.

## 2. Experimental

### 2.1 Optical system development and alignment simulation

Fig.1 is a schematic of the experimental optical system designed and developed for multiple laser beam generation and delivery to a single cylinder IC test engine. Fig.2 illustrates the engine system comprising engine, diagnostics and data acquisition. As shown in Fig.1, the laser used was a flashlamp-pumped Q-switched Nd:YAG laser (Litron LPY 764-30), delivering up to 500mJ output energy at a wavelength of 532 nm. The SLM used was a LCoS device (Hamamatsu X10468) with 800×600 pixels and dielectric coating for 532 nm operation (reflectivity > 99%). Computer generated holograms (CGHs) were displayed on the SLM to create multi-beam patterns by diffraction [12-15]. ZEMAX optical modelling software was used for optical design and simulation of beam alignment and propagation performance. 1×2 and 1×3 beam arrays were generated using binary linear grating CGHs. Arrays with higher numbers of beams (e.g. 1×5) were created using Dammann grating CGHs [14, 15], according to the grating equation:

$$d(sin\theta_i + sin\theta_m) = m\lambda \tag{1}$$

$$\theta_m = \arcsin(\frac{m\lambda}{d} - sin\theta_i) \tag{2}$$

where $d$ is the grating period, $\theta_i$ is incident angle at the SLM, $m$ is the diffracted order number and $\theta_m$ is the corresponding angle of diffraction. $\theta_m$, and hence the separation of the multiple foci, can be adjusted by varying the correspondent grating period ($d$). After the SLM, the laser beam was passed through a series of lenses and mirrors forming a ×2 Keplerian telescope (lens 1&2) and two 4$f$ optical systems (lens 3&4, lens 5&6 in dummy line, and lens 5'&6' in engine line). These optical systems reduced the laser beam diameter and reconstructed the optical plane from A (SLM) to A' (end of the 'dummy line') and A'' (the end of 'engine line'). This arrangement sought to ensure that the multi-beam patterns were delivered to the engine cylinder without clipping. As shown, a 'dummy line' was designed to make the laser ignition pattern visible outside the engine. The conditions for both the engine and dummy line match, since the laser propagation from J to A' (dummy line) mimics the propagation from J to A'' (engine line). The multi-beam pattern was then passed through an optical plug containing a 2 mm thick plano-convex sapphire lens ($f$ = 16 mm) to generate the multiple foci. To create multiple sparks, the optical set up was designed to achieve

focused intensities exceeding $10^{11}$ $Wcm^{-2}$ in each of the transmitted beams, sufficient to cause dielectric breakdown of the air-fuel mixture [9-11].

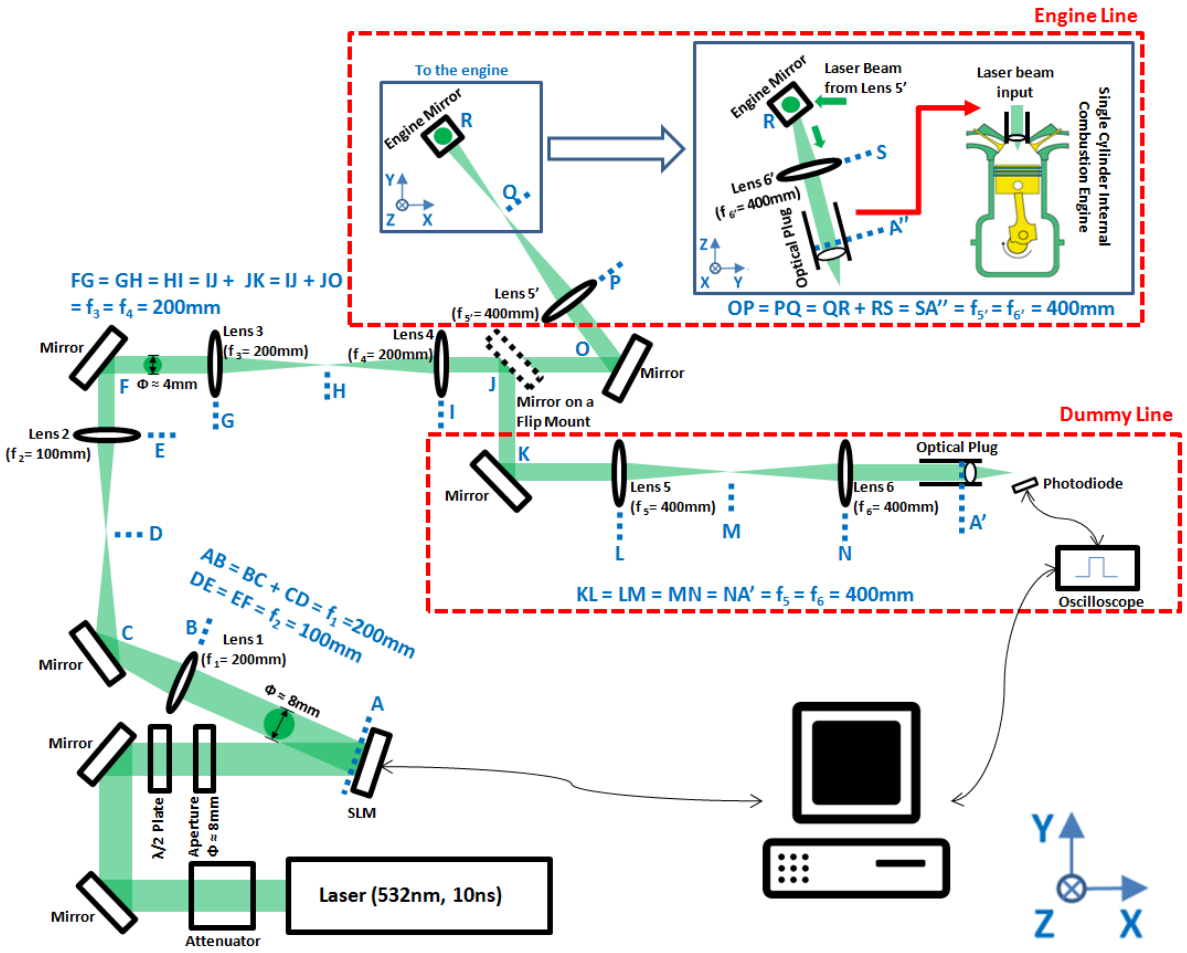


Fig. 1: Experimental setup – Optical system for multi-beam generation and delivery to the test engine

### 2.2 SLM optical damage test

Prior to any SLM experiments involving high laser pulse energy ($E_p$) input, optical damage experiments were carried out to determine a safe threshold input energy for the SLM, using LCoS samples provided by SLM maker Hamamatsu Photonics. All LCoS samples had the same material and coating as the SLM. A laser beam of diameter ≈ 8 mm, with various values of $E_p$ (increasing from 10 mJ), was applied to each one of the samples for a period of 10mins. In each case, if the sample appeared unaffected (i.e. undamaged) by the irradiation, the energy $E_p$ was then increased by 10 mJ and applied to the sample for a further 10mins. This process was repeated, gradually increasing $E_p$, until damage became evident.

### 2.3 Stability analysis of laser induced sparks generated in multiple foci (Dummy line)

To determine the minimum energy needed for spark creation under the optical conditions set out in Fig.1, and hence how many multiple beams with sufficient energy could be applied for engine LI, an experiment was carried out to analyse the sparking stability of multiple laser beam generated by the SLM. As in Fig.1, a photodiode connected to an oscilloscope was placed near to the optical plug in the dummy line optical train, to capture light emitted from plasma formation in the spark. The captured signals were recorded to show if breakdown had taken place or not, while the probability of breakdown plasma formation was then

measured as the pulse energy was increased. The same diagnostic was used in engine LI experiments to indicate any misfires occurring, by capturing ignition light emitted back through the optical plug.

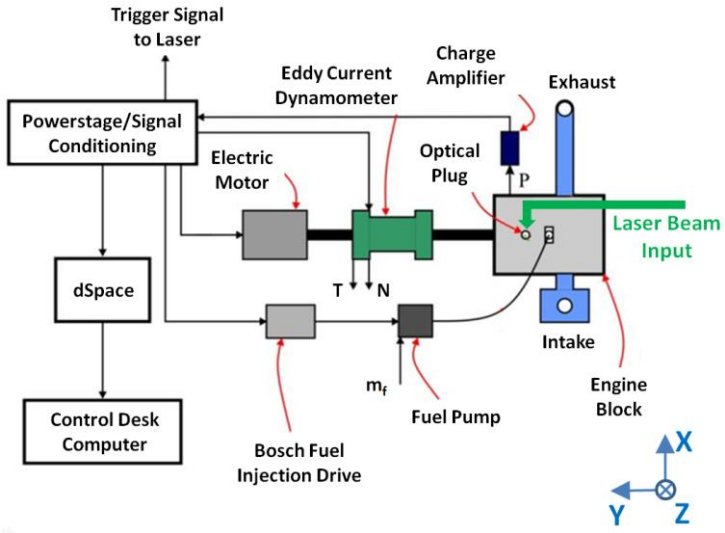


Fig. 2: Experimental setup – test engine, diagnostics and data acquisition [16]

### 2.4 Single cylinder IC test engine and LI experiments

The arrangement of engine, diagnostics and data acquisition is shown in Fig.2. The engine used was a prototype single cylinder gasoline engine with 776 cc swept volume, compression ratio of 9.2 and 100 bar pressure direct injection fuel delivery. A dSPACE prototyping system was designed for engine control and data acquisition, with a signal from this used to externally trigger the laser output in synch with the engine cycle [16]. Operating in 'spark advance' mode, the ignition timing was set at ~ 20° 'before top dead centre', late in the compression stroke, when the cylinder volume would have dimensions 102 mm diam. by ~ 15 mm height. The engine diagnostics included a pressure sensor (AVL M5) and charge amplifier (Kistler 5011), used for sensitive measurement of in-cylinder pressure. The attached dynamometer was used to measure engine power output, accounting for losses. The following brief definition of parameters used later in characterising engine performance may benefit readers not familiar with engine technology. The Indicated Mean Effective Pressure (*IMEP*) is a theoretical expression for the mean pressure exerted on the piston during the expansion stroke of a cycle (ignoring friction), and is defined as [17]:

$$IMEP = \frac{W_i}{V_d} \tag{3}$$

where $V_d$ is the displaced cylinder volume and $W_i$ is the gross work delivered to the piston over the compression and expansion strokes, which is obtained by the circular integration of the pressures, $P$, over these strokes, with respect to cylinder volume [17]:

$$W_i = \oint PdV \tag{4}$$

*IMEP* is extensively used in engine calibration and the coefficient of variation in *IMEP* ($COV_{IMEP}$) is used as an indicator of combustion stability. The $COV_{IMEP}$ is commonly used in industry and is defined as [17]:

$$COV_{IMEP} = \frac{\sigma_{IMEP}}{IMEP_{mean}} \times 100\% \tag{5}$$

where $\sigma_{IMEP}$ is the standard deviation in *IMEP* and $IMEP_{mean}$ is the mean *IMEP*. The $COV_{IMEP}$ is expressed as a percentage and defines the variability in indicated work per cycle.

## 3. Results, analysis and discussion

### 3.1 Optical alignment simulation

Fig.3 shows optical designs for (a) the dummy line and (b) engine line, arrived at via ZEMAX modelling.

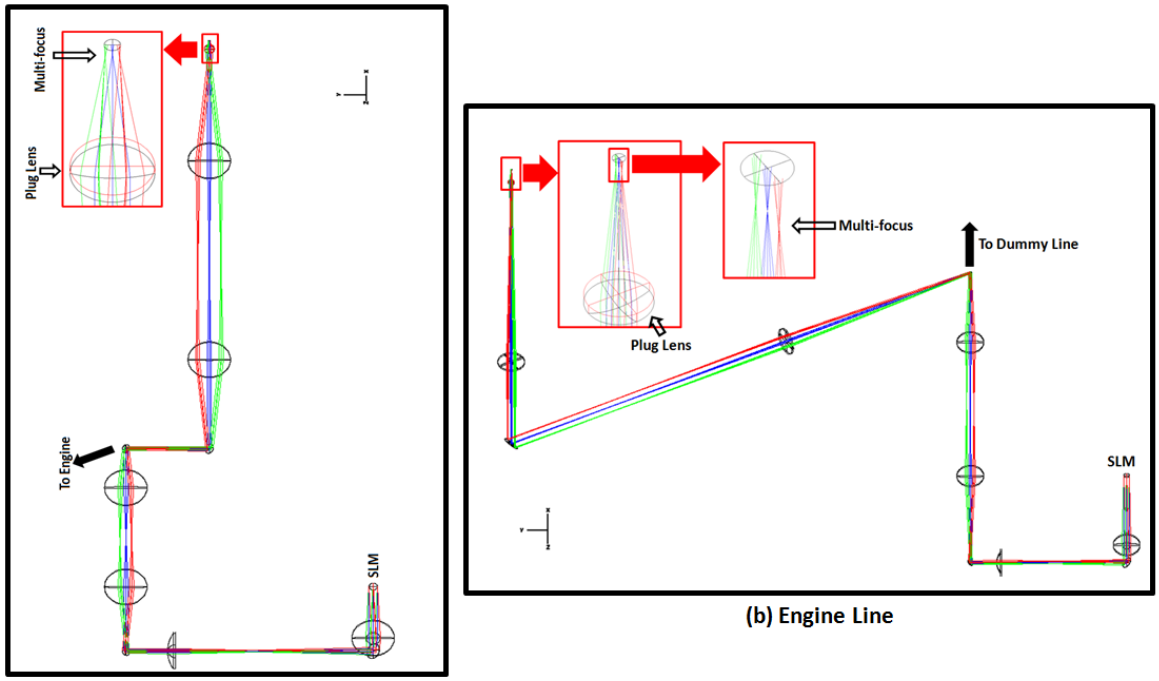


Fig. 3: ZEMAX modelling of the experimental optical alignment

As shown, the multi-beam pattern propagated through the designed optical system and reached the plug lens without clipping. Based on the models, an experimental setup was created on an optical table next to the engine. Fig.4 shows some optical alignment photographs taken of the propagating laser beams (the vicinity of the room was sprayed with small particles to make the beams visible). As this shows, the multi-beam patterns were delivered to the dummy line (a) and to the engine (b) without clipping. All the optics used had correct dielectric coating for 532nm. The energy losses through the optical system were < 5%.

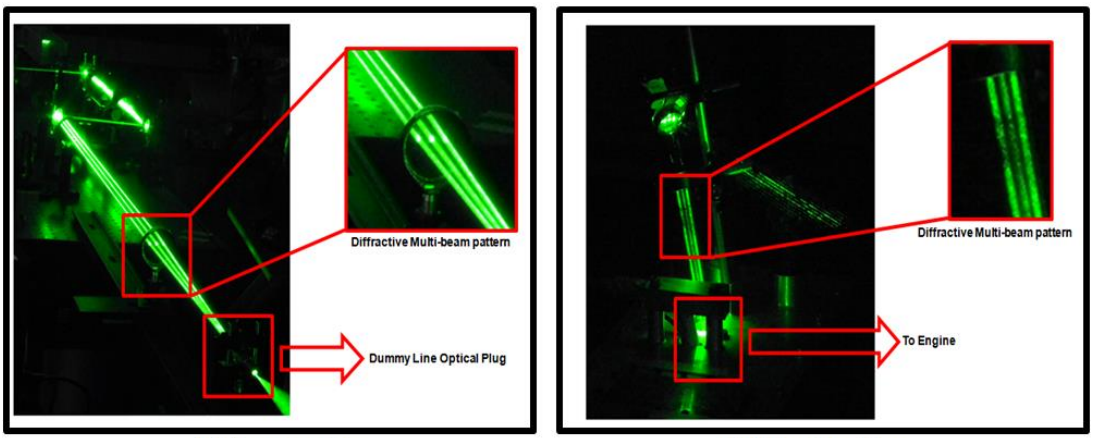


Fig. 4: Multi-beam delivery through the optical plug without clipping: (a) dummy line; (b) (vibrating) engine

### 3.2 SLM optical damage experiments

The results are given in Table 1. As shown, the LCoS sample was damaged when $E_p$ reached a value between 80mJ and 86mJ. This value of damage threshold, $E_{p\text{-}th}$ was found to vary slightly when changing the laser repetition rate ($R$). When $R$ = 10Hz or 15Hz, $E_{p\text{-}th}$ was the highest (≈ 86mJ). This is because the Litron laser was designed to give its best beam mode at frequencies between 10Hz and 15Hz. The $E_{p\text{-}th}$ decreased slightly when $R$ was either too low, at 1Hz or 5Hz, or too high, at 20Hz or 25Hz, due to the poorer beam mode and possibly also hot spots caused by thermal lensing effects. $E_{p\text{-}th}$ was lowest (80mJ) when R = 30Hz, most probably due to the higher average power in addition to the poorer beam mode.

Table.1: Optical damage results for LCoS samples

| $E_p$(mJ) \ R(Hz) | 1 | 5 | 10 | 15 | 20 | 25 | 30 |
|---|---|---|---|---|---|---|---|
| 78 (F≈39mJ/cm$^2$) | | | | | | | |
| 80 (F≈40mJ/cm$^2$) | | | | | | | |
| 82 (F≈41mJ/cm$^2$) | | | | | | | |
| 84 (F≈42mJ/cm$^2$) | | | | | | | |
| 86 (F≈43mJ/cm$^2$) | | | | | | | |

Normal: Damaged:

Fig 5 shows an example of damage to the LCoS that can be caused by pulse energies exceeding $E_{p\text{-}th}$. To avoid such costly damage, applying ~ 25% safety margin, the input laser energy was limited to 60mJ.

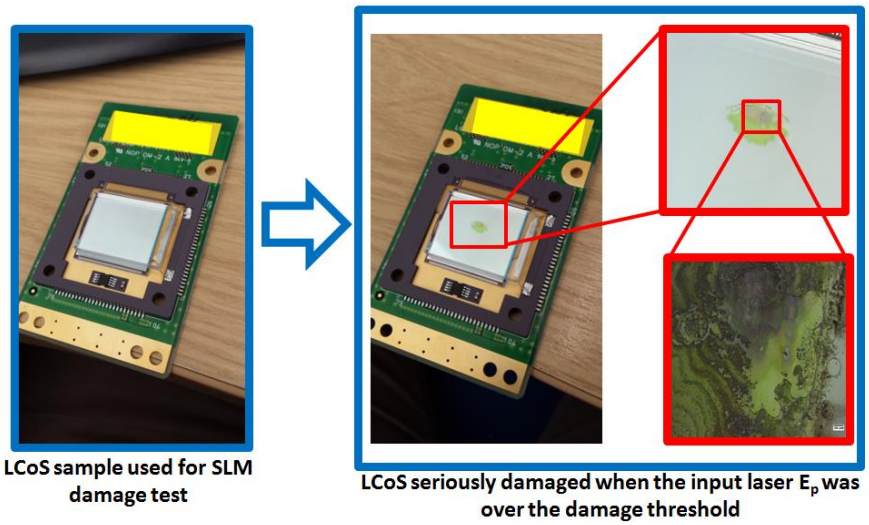


Fig. 5: SLM optical damage – visual inspection of LCoS samples

### 3.3 Stability analysis of laser induced sparks generated in multiple foci (Dummy line)

With the pulse energy of the laser adjusted to 60mJ (measured close up to the SLM) and a repetition rate of 10Hz, multi-location sparks were successfully generated on the dummy line. As can be seen in the first column of images in Fig.6, an intense single laser induced spark was created when no CGH was applied. The other three columns show the laser beam split into two, three and five identical diffracted beams respectively, when applying corresponding binary linear grating CGHs. Row (a) shows the binary gratings displayed on the SLM, row (b) the far-field beam profile after the SLM and row (c) the sparks created after the optical plug. Spark generation was observed for one to three beam foci (the first three columns). In contrast, the five beam foci case (fourth column) shows no sparks after the optical plug, due to the fact that insufficient energy was assigned to the individual diffracted order to generate an air-breakdown spark when the laser beam was split into five.

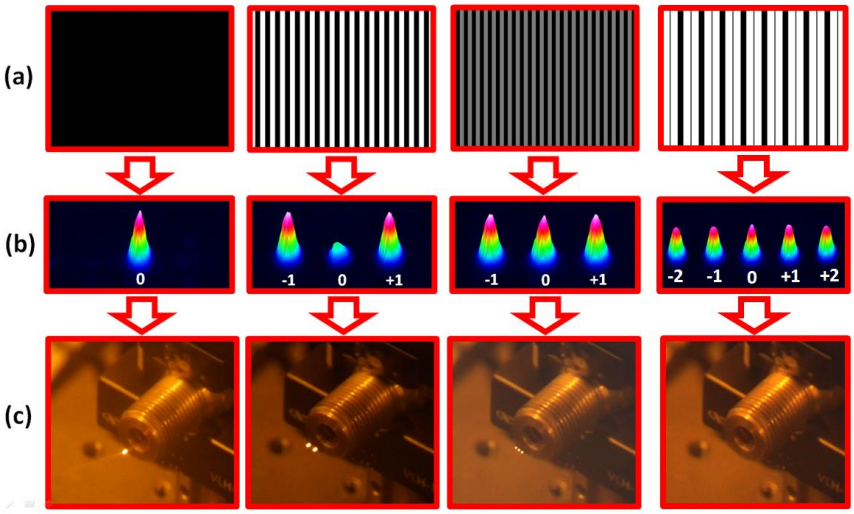


Fig. 6 Laser induced multiple sparks created by binary Dammann grating CGHs: (a) gratings displayed on the SLM; (b) far-field beam profile after the SLM; (c) sparks created after the optical plug

The traces presented in Fig.7 are a sample of photodiode data capturing plasma formation events in the cases of single-location, two-location and three-location sparking. These show that the single- and two-location sparks were perfectly stable; whereas, the three-location sparks were irregular.

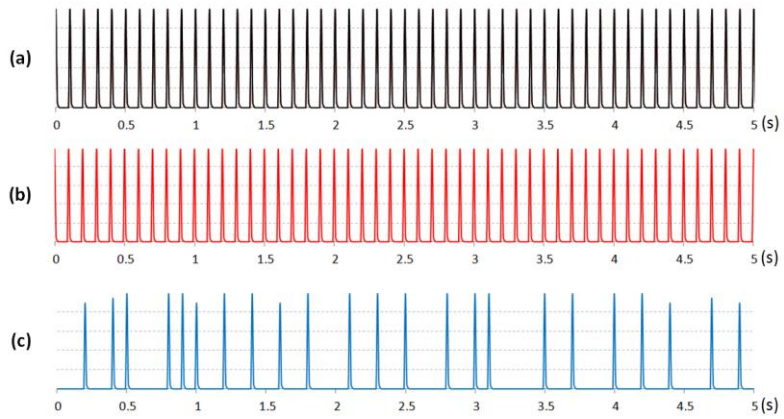


Fig. 7: Sample of photodiode data capturing plasma formation events (a) single-location sparking, (b) two-location sparking, (c) three-location sparking

A graph of breakdown plasma formation probability versus input energy $E_p$ (single beam) was plotted, as shown in Fig.8, to gain an understanding of the relationship between the two parameters. The formation probability was calculated by simply taking the ratio between the number of peaks in the photodiode measurement and that of the trigger signal. The onset of breakdown spark generation took place when $E_p$ reached 18mJ (running at $R$ = 10Hz) and became stable (i.e. 100% probability of plasma formation) when $E_p$ reached approximately 22mJ. When the laser was split into two beams, the $E_p$ of individual spark locations was measured to be ≈ 27mJ, which is higher than the $E_p$ required for 100% probability of plasma formation, hence demonstrating the stable sparking. However, when the laser was split into three beams, the $E_p$ was measured to be only about 19.5mJ for each spot, lower than the $E_p$ required for 100% probability of plasma formation, hence resulting in unstable sparking. This finding led to the selection of dual-position LI for comparison with single-location LI for the engine performance tests.

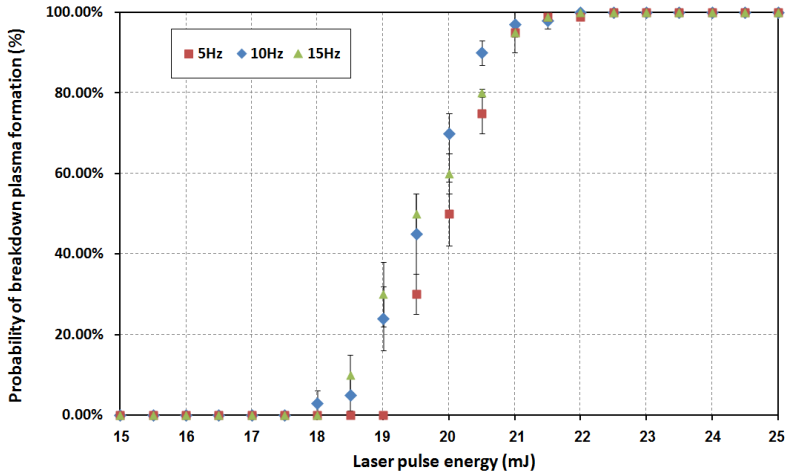


Fig. 8: Stability of plasma formation versus laser pulse energy at pulse frequencies of 5, 10 and 15Hz.

The lateral spacing of individual sparks could be varied arbitrarily by modifying CGHs applied to the SLM [12]. Fig.9 shows captured images of dual-location sparks with lateral spacing ($d$) of ~ 4, 2 and 1 mm,

obtained by adjustment of the CGH grating period (as discussed in section 2.1). The single beam spark is shown for comparison. The diffraction efficiency varied by < 2% as the spacing was changed, so the energy per spark had the same maximum percentage variation. For 60mJ onto the SLM, the energy per foci was kept at ~ 27 mJ to ensure excellent sparking stability (100% probability of plasma formation). The spacing $d$ ~ 4 mm was then selected for engine LI experiments, so that engine performance data for dual-location LI could then justifiably be said to be the result of a clear spatial separation of the 2 simultaneous sparks, within the cylinder volume (10.2 cm bore), sharing the total energy equally between them.

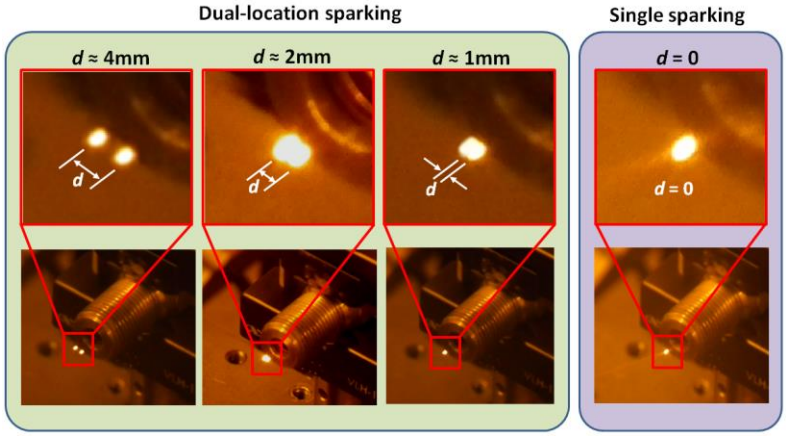


Fig. 9: Dual-location laser-induced sparks with varying lateral spacing, alongside a single beam case

### 3.4 Single- and dual-location LI experiments on the single cylinder IC test engine

Fig. 10 compares in-cylinder pressure traces for single- and dual-location ($d \approx 4$ mm) LI, at an air-fuel ratio $\lambda \approx 1.2$. This leaner air-fuel ratio was chosen since one of the advantages of laser over spark ignition is leaner engine running, which is more fuel efficient. In both the single- and dual-location cases the total laser energy input to the cylinder was the same. For the dual-location, the 2 sparks each had the same amount of energy.

The data plotted was recorded in real time, with the engine running at a constant speed of ~ 1000 rpm (ignition frequency ≈ 8.33Hz). Each data point recorded at every 1° of crank angle represents ~ 500 engine cycles. These pressure traces show dual-location LI gave improved engine stability. At the moment of ignition, the fuel distribution might not be perfectly homogenous, some areas might still be stratified. If the spark location happens to be one of these areas, then the probability of ignition is reduced, which could explain why dual-location LI misfires less.

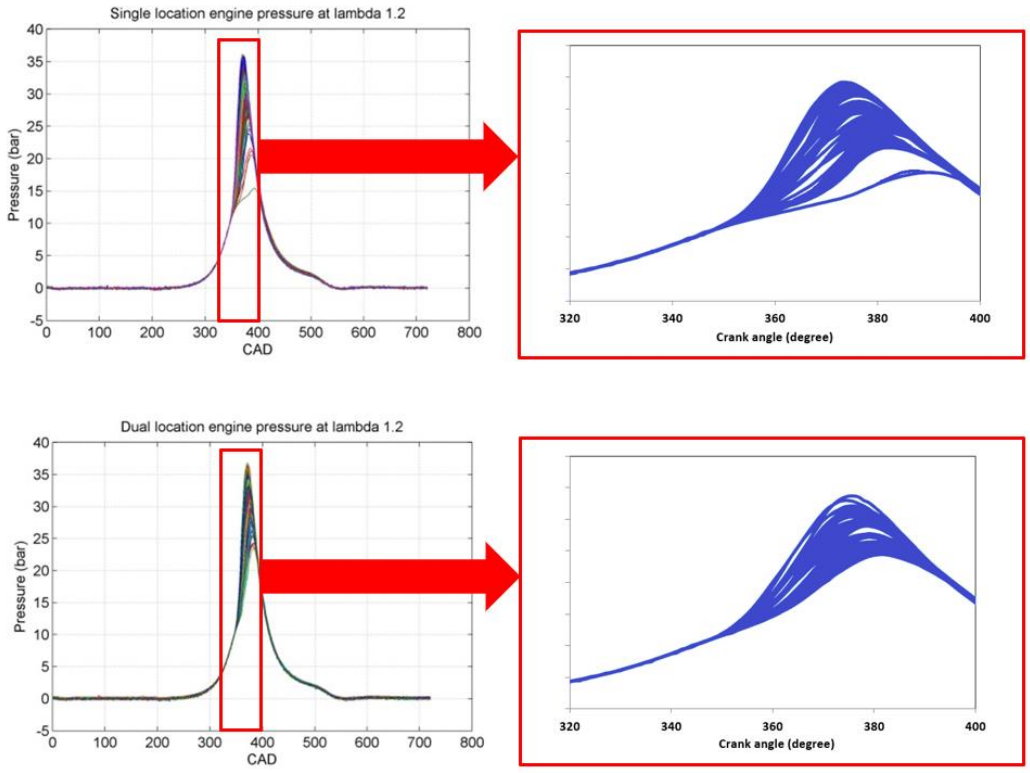


Fig. 10: Comparison of pressure traces (in-cylinder pressure versus crank angle in degrees) for single- and dual-position (4mm spacing) laser ignition of a single cylinder engine at air-fuel ratio $\lambda \approx 1.2$.

Fig.11 shows sample data acquired by photodiode sensing of light emission during engine operation with both single- and dual-location LI at $\lambda \approx 1.2$. In (a), evidence of misfires can be seen for the case of single-location LI; whereas, in (b), no misfires were observed for the case of dual-location LI.

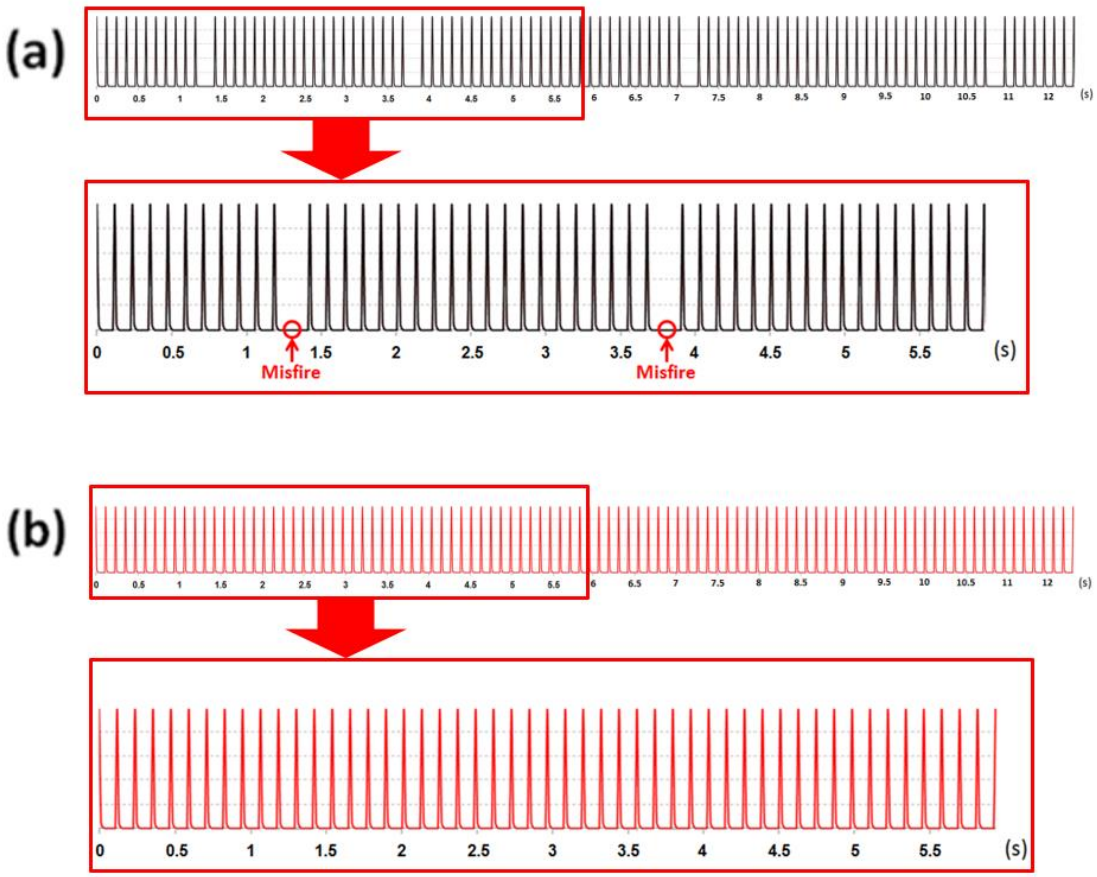


Fig. 11: Sample photodiode signals from (a) single-location and (b) dual location engine LI at $\lambda \approx 1.2$

Fig.12 compares the percentage of misfires, plotted against air-fuel ratio ($\lambda$), between single- and dual location LI. Photodiode detection of light emitted from the combustion chamber back through the optical plug was used to record numbers of combustion and misfire events, from which the percentage misfires was calculated. As can be seen, dual location LI gave less misfires than single location LI for all $\lambda$ values >1.05. It is worth pointing out here, even with single-location LI, the ability to operate this engine at an air-fuel ratio of 1.45 (albeit with > 30 % misfires) is an impressive and encouraging achievement for LI. With conventional electric SI, the engine could not run properly at values of $\lambda$ higher than ~ 1.2.

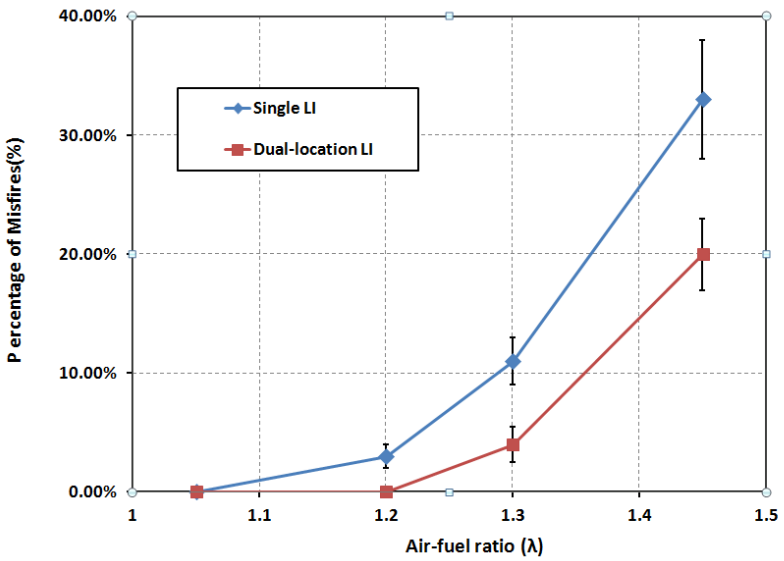


Fig.12: Percentage of misfires against air-fuel ratio ($\lambda$) for single- and dual-location LI.

Figs. 13 and 14 show the variation in engine output power and $COV_{IMEP}$, measured respectively against increasing air-fuel ratio ($\lambda$). The graphs are presented in this order because values of $COV_{IMEP}$ are derived using values of the generated power. Compared to single-location LI, dual-location LI leads to higher engine power output and reduced $COV_{IMEP}$ (better engine stability) when operating with increasingly lean mixtures. This was attributed to the two simultaneous separate laser sparks within the combustion volume reducing the probability of misfires, as the air-fuel mixture became increasingly leaner. Though not included here in the presented data, the engine losses were also reduced for the dual-location LI case, with less unburnt fuel and emissions. A higher output power generated (for dual-location LI) means the air-fuel mixture burnt more fully and at a more optimised rate, therefore the variation of force on the piston matched better what was needed in the engine cycle. The findings of our recent LI studies indicate that lower $COV_{IMEP}$ correlates with lower NOx emissions [16].

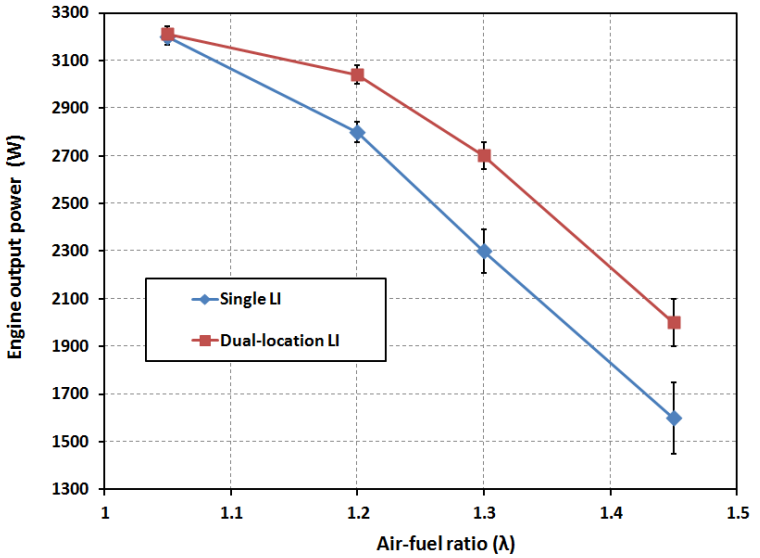


Fig.13: Engine output power vs Air-fuel ratio ($\lambda$) for single- and dual-location LI.

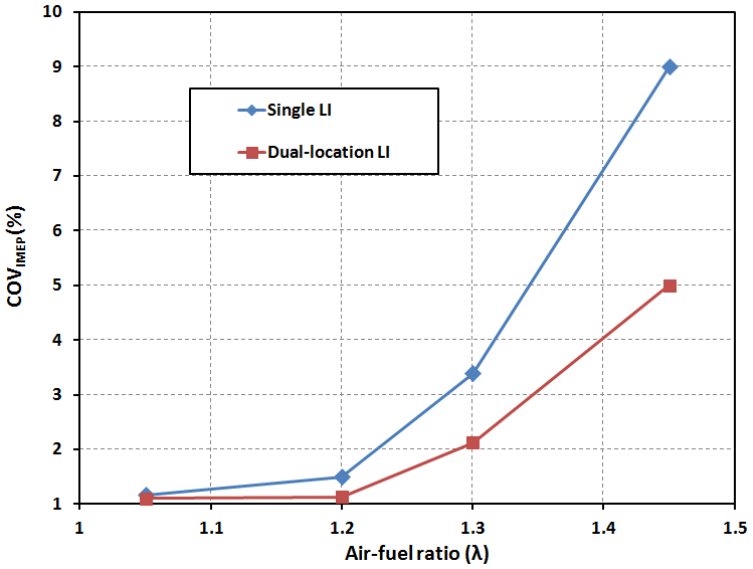


Fig.14: $COV_{IMEP}$ vs Air-fuel ratio ($\lambda$) for single- and dual-location LI.

The findings here of improved engine performance with simultaneous dual-location LI are considered to be important for future LI system development and exploitation. With a matrix of suitable laser and optical parameters identified to match a range of desirable engine running conditions (including cold start, idling, etc.), cost-effective miniaturised LI systems and standardised optics could then be developed to supplant such a research system as described here. The LCoS response characteristic enables CGHs applied to the SLM to be refreshed at rates of up to 50-60 Hz, so the distribution of laser energy within the cylinder can actually be freely varied in 'real time' (at every engine cycle).

## 4. Conclusions

We have reported here on experiments and results from a study on multi-location LI of a single cylinder IC engine using a SLM. Multi-beam diffracted patterns were successfully created by applying CGHs to a LCoS SLM. An optical system incorporating the SLM was successfully designed and developed, using ZEMAX optical design modelling software, for efficiently delivery of multi-beam patterns into the engine without clipping. An optical damage experiment was carried out on LCoS samples provided by the SLM maker, from which a safe limit threshold of 60 mJ laser pulse energy input to the SLM was determined. The sparking probability of multi-beam foci was studied and its variation with laser pulse energy analysed using a photodiode light sensor. Diffracting this into three identical beams gave slightly insufficient energy to guarantee 100% sparking, so two equal energy beams (dual-position) were selected for subsequent engine experiments. Applying appropriate CGHs to SLM, the spacing between these dual-position sparks could be freely varied from 1-4 mm. By selecting a spacing of 4 mm for the engine LI experiments, engine performance results for dual-location LI could be justifiably attributed to a clear spatial separation of the 2 simultaneous sparks within the combustion volume. Comparing between single- and dual-location LI, the results showed clearly that dual-location LI gave more stable combustion and higher power output when operating with increasingly lean air-fuel mixtures. This was attributed to the simultaneous generation of two separate laser sparks within the combustion volume giving reduced probability of misfires, especially for increasingly leaner air-fuel mixtures. Engine losses were also reduced for the case of dual-location LI, with less unburnt fuel and emissions. Successful engine operation (despite misfires) by LI at air-fuel ratios up to 1.45 goes well beyond the typical SI limit ($\lambda$ ~ 1.2) for this test engine. These findings are deemed to be important for future LI system development and implementation.

**Acknowledgments**

The authors wish to acknowledge the UK's Engineering & Physical Sciences Research Council (EPSRC), together with industry project partners Ford Motor Company and Cambustion Ltd, for their funding and technical support of research on laser ignition at the University of Liverpool (EPSRC grant reference: EP/J003573/1). The authors would also like to acknowledge the kind support from Jack Bennett (Senior Sales Engineer, Hamamatsu Photonics) in providing LCoS samples for the SLM optical damage tests.

**References**

[1] Ronney PD, Laser versus conventional ignition of flames, Opt. Eng. 1994; 33: 510–22.
[2] Weinrotter M, Srivastava D K, Iskra K, Graf J, Kopecek H, Klausner J, Herdin G, Wintner E, Laser ignition of engines - a realistic option!, Proc. SPIE 2006; 6053: 605316.
[3] Phuoc TX, Laser-induced spark ignition fundamental and applications, Opt. Lasers Eng 2006; 44: 351–97.
[4] Alger TA, Mehta D Chadwell CJ, Laser ignition in a pre-mixed engine: the effect of focal volume and energy density on stability and the lean operating limit, In: SAE Technical Papers, Powertrain Fluid Syst. Conf. Exhibition (San Antonio 24–27 October) 2005.
[5] Mullett JD, Dodd R, Williams CJ, Triantos G, Dearden G, Shenton AT, Watkins KG, Carroll SD, Scarisbrick AD, Keen S, The influence of beam energy, mode and focal length on the control of laser ignition in an internal combustion engine, J. Phys. D: Appl. Phys. 2007; 40: 4730–9.
[6] Weinrotter M, Iskra K, Al-Janabi AH, Kopecek H, Wintner E, Laser ignition of engines: multipoint, fiber delivery and diagnostics, Proc. SPIE 2005; 5850: 88–9.
[7] Morsy MH, Chung SH, Laser-induced multi-point ignition with a single-shot laser using two conical cavities for hydrogen/air mixture, Exp. Therm. Fluid Sci. 2003; 27: 491–7.
[8] Pavel N, Tsunekane M, Taira T, Composite, all ceramics, high-peak power Nd:YAG/Cr4+:YAG monolithic micro-laser with multiple-beam output for engine ignition, Opt. Express 2011; 19: 9378–84.
[9] Tauer J, Kofler H, Wintner E, Laser-initiated ignition, Laser Photon. Rev. 2010; 4: 99–122.
[10] Morsy MH, Review and recent developments of laser ignition for internal combustion engine applications, Renew. Sust. Energ. Rev. 2012; 16: 4849–75.
[11] Dearden G, Shenton T, Laser ignited engines: progress, challenges and prospects, Opt. Express 2013; 21: A1113–25.
[12] Lyon E, Kuang Z, Cheng H, Page V, Shenton T, Dearden G, Multi-point laser spark generation for internal combustion engines using a spatial light modulator, J. Phys. D: Appl. Phys. 2014; 47: 475501.
[13] Leach J, Wulff K, Sinclair G, Jordan P, Courtial J, Thomson L, Gibson G, Karunwi K, Cooper J, Laczik ZJ, Padgett M, Interactive approach to optical tweezers control, Appl. Opt. 2006; 45: 897-903.
[14] Dammann H, Gortler K, High-efficiency in-line multiple imaging by means of multiple phase holograms, Optics Communications 1971; 3: 312–5.
[15] Kuang Z, Perrie W, Liu D, Edwardson S, Jiang Y, Fearon E, Watkins K, Dearden G, Ultrafast laser parallel microprocessing using high uniformity binary Dammann grating generated beam array, Applied Surface Sci. 2013; 273: 101-6.
[16] Cheng H, Kuang Z, Page V, Lyon E, Shenton T, Dearden G, Multiple Pulse Laser Ignition in GDI Lean Combustion, International Journal of Powertrains 2015; 5: 55-68.
[17] Heywood J, Internal combustion engine fundamentals, McGraw-Hill, New York, 1998.